JACS
JOURNAL OF THE AMERICAN CHEMICAL SOCIETY

Communication

pubs.acs.org/JACS

Synthesis and Liquid-Crystal Behavior of Bent Colloidal Silica Rods

Yang Yang,[†,‡] Guangdong Chen,[‡] Luz J. Martinez-Miranda,[§] Hua Yu,[†] Kun Liu,[*,†] and Zhihong Nie[*,‡]

[†]State Key Laboratory of Supramolecular Structure and Materials, College of Chemistry, Jilin University, Changchun 130012, China
[‡]Department of Chemistry and Biochemistry and [§]Department of Materials Science and Engineering, University of Maryland, College Park, Maryland 20742, United States

Supporting Information

ABSTRACT: The design and assembly of novel colloidal particles are of both academic and technological interest. We developed a wet-chemical route to synthesize monodisperse bent rigid silica rods by controlled perturbation of emulsion-templated growth. The bending angle of the rods can be tuned in a range of 0−50° by varying the strength of perturbation in the reaction temperature or pH in the course of rod growth. The length of each arm of the bent rods can be individually controlled by adjusting the reaction time. For the first time we demonstrated that the bent silica rods resemble banana-shaped liquid-crystal molecules and assemble into ordered structures with a typical smectic B2 phase. The bent silica rods could serve as a visualizable mesoscopic model for exploiting the phase behaviors of bent molecules which represent a typical class of liquid-crystal molecules.

Colloidal particles are of particular interest because of their broad applications, e.g., in coating, sensing, and photonic crystals.[1] Assembly of colloidal particles into ordered architectures[2] is essential for engineering new functional materials[3] and devices.[4] Owing to their unique dimension (from hundreds of nanometers to micrometer scale), colloidal particles can often be directly visualized under an optical microscope. This makes them ideal models for studying the assembly or phase behavior of atoms and molecules that are otherwise not easy to observe directly.[5] For instance, spherical colloids are frequently used to understand the packing and dynamics of atoms.[6] To achieve new insight into the interaction and self-assembly of molecules in general, colloidal particles with nonspherical shapes (e.g., platelets, bowls, and rods) will be required, given the geometric diversity of organic molecules.[7] In particular, colloidal rods are considered as a prominent model for rodlike small molecules.[8] The orientational and positional ordering phases of rods are strongly dependent on the aspect ratio and density of rods.[8a−e]

Bent or banana-shaped molecules have attracted great attention in, e.g., mesogenic materials and supramolecular chemistry over the past decades.[9] Because of the characteristic packing and spontaneous polarization, several unconventional liquid-crystal (LC) phases (e.g., chiral cholesteric phases, blue phases, ferroelectric/antiferroelectric smectic and columnar phases) are observed for bent rodlike molecules. They show potential applications in electrooptic devices, nonlinear optics, thermochromism, etc.[10] Available colloidal analogues of organic molecules are largely limited to spheres, platelets, bowls, or cylindrical rods because of synthetic challenges.[11] Bent colloidal rods show promise in various fields, e.g., nanoantennas, split-ring resonators, and biomimetic motion.[12] To date, bent rods could only be prepared by top-down approaches like templated electrochemical deposition and electron-beam lithography.[12,13] However, these methods are fairly expensive and time-consuming and usually result in low yields. We are motivated to develop an efficient low-cost wet-chemical synthetic method to fabricate bent colloidal rods and study their assembly behaviors.

Recently, a wet-chemical methodology was developed for the controlled synthesis of highly monodispersed silica rods by several groups, including ours.[8a,f,14] In this synthesis, the hydrolysis and condensation of tetraethoxysilane (TEOS) at the interface of water emulsions lead to the anisotropic growth of silica rods tightly bound to one side of the emulsion in the presence of a structure-directing agent. Inspired by recent research,[8a,14b] we present a novel synthetic strategy to produce monodisperse bent silica rods (BSRs) with tunable bending angle (α) and length (L) of each arm. This one-pot synthetic strategy utilizes temperature or pH variation to perturb the emulsion attached at one end of the rods and hence to induce the deviation of otherwise straight growth of silica rods to generate BSRs (Scheme 1a). The α of BSRs can be tuned in a range of 0−50° by alternating the pH or reaction temperature during the growth of the rods. For the first time, we demonstrate that the BSRs

Scheme 1. (a) Synthesis of BSRs through Temperature or pH Modulation[a] and (b) Assembly of BSRs into Smectic B2 Phase

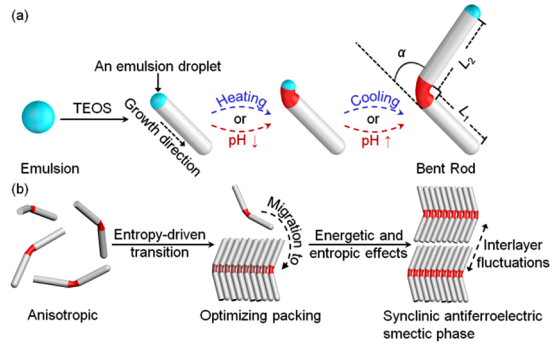

[a]Hydrolysis of TEOS is initiated at the surface of a water emulsion to induce anisotropic growth of the first straight block of BSRs. Upon heating or reducing pH, the perturbation of the emulsion droplets results in a curved segment. Further hydrolysis at original temperature or pH leads to the growth of the second straight block of BSRs.

Received: November 4, 2015
Published: December 23, 2015

DOI: 10.1021/jacs.5b11546
J. Am. Chem. Soc. 2016, 138, 68−71

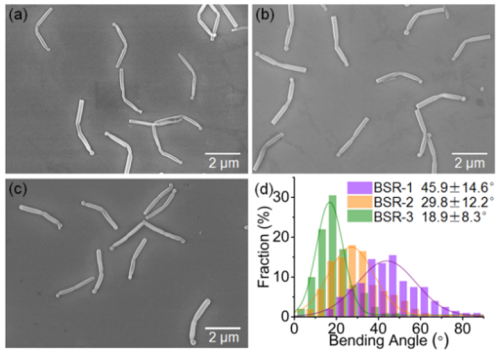

Figure 1. Representative SEM images of BSRs with different bending angles through temperature modulation. Perturbation conditions were (a) 65 °C for 5 min for BSR-1, (b) 45 °C for 20 min for BSR-2, and (c) 35 °C for 30 min for BSR-3. Reaction conditions for growing two straight blocks of all the BSRs were 25 °C for 2 h before temperature perturbation and 25 °C for 4 h after temperature perturbation. (d) Bending angle distribution of BSR-1, BSR-2, and BSR-3 is obtained by counting 200 rods for each sample.

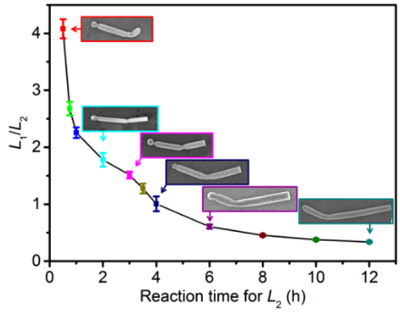

Figure 2. Dependence of length ratio of the first straight block (L_1) to the second straight block (L_2) of BSRs on reaction time for the second block. The first blocks were all grown at 25 °C for 2 h, and the perturbations were all at 45 °C for 20 min. Insets: Corresponding SEM images of synthesized BSRs.

resemble banana-shaped molecules and self-assemble into LCs with typical synclinic tilted antiferroelectric (AF) smectic bow phase (SmC_SP_A) in B2 phase (Scheme 1b).[15]

The BSRs were synthesized by consecutive hydrolysis and condensation of TEOS at alternating temperature or pH of the reaction system. Taking temperature-induced formation of BSRs as an example, a mixture of water, ethanol, sodium citrate, and ammonia (NH_3) was added into a solution of polyvinylpyrrolidone (PVP, structure-directing agent) in *n*-pentanol (see details in Supporting Information). The solution was vigorously shaken to form water-in-pentanol emulsions. The silica precursor of TEOS was then added into the solution. Hydrolysis and condensation of TEOS at 25 °C produced the first straight block of BSRs. The diameter (D) of the first block was ~200−300 nm, the same as that of straight rods reported previously (Figure S1).[8a] The matchstick-like structures may result from the rapid hydrolysis and condensation of partially hydrolyzed TEOS.[16] The length of the first block can be varied from 700 nm to 2 μm by controlling the hydrolysis time (Figures S2 and S3). During the growth, increasing the reaction temperature from 25 to >35 °C produced a curved segment with $D \approx 130-180$ nm at the end of the first straight block. The reaction system was then cooled back to room temperature for the further growth of the second straight block to produce BSRs (Figure 1).

The bending angle of the rods can be tuned by controlling the reaction temperature. The higher the temperature during the perturbation period of time, the larger the α of the resulting rods (Figures 1 and S3), due to the smaller emulsion droplets at higher temperature. When the perturbation temperature was set at 65 °C, the average α was 45.9 ± 14.6° (Figure 1a,d). For a lower perturbation temperature of 45 °C, the average α was reduced to 29.8 ± 12.2°, and the bending angles became more uniform (Figure 1b,d). Further reducing the perturbation temperature to 35 °C led to rods with α = 18.9 ± 8.3° and further improved homogeneity (Figure 1c,d). However, when the perturbation temperature was >70 °C, the synthesis did not produce BSRs with further increased α. Instead, the α distribution of the rods became broader, presumably due to the fast hydrolysis and condensation of TEOS at high temperature (Figure S4). Moreover, the curvature of the BSRs' corners (i.e., bending region) could be increased by reducing the time of temperature perturbation (Figures 1, S3, and S5). By gradually increasing the temperature, banana-shaped curved rods can be obtained (Figure S6). Lowering the reaction temperature back to 25 °C led to the second straight block. The second straight block had the same D as the first block since the water emulsions were restored to their original size.

By changing the growth time of the second block, both symmetric and asymmetric BSRs can be produced (Figure 2). The growth condition for the first straight block of all BSRs was set at 25 °C for 2 h, and the perturbation period was 20 min at 45 °C. In this case, the length ratios of the first straight block to the second straight block (L_1/L_2) can be tuned from ~4.0 to 0.3 by manipulating the reaction time for L_2. Particularly, symmetric BSRs with two blocks of the same length can be obtained only when the reaction time for L_2 was 4 h, twice that for L_1. Growth of the L_2 block stopped after 12 h, probably due to the loss of "living" activity: further prolonging the reaction time for L_2 could not increase the length ratio of two blocks.

To understand the bending mechanism of BSRs, we explored the growth kinetics of rods at different stages of the synthesis. A close inspection of the process shows that the variation in temperature perturbs the emulsion droplet, which serves as the template for the anisotropic growth of rods.[8a] The ability to visualize emulsion droplets by transmission electron microscopy (TEM) under high vacuum can be attributed to a high concentration of PVP in the emulsion droplets. Upon evaporation of water, dried PVP serves as a staining agent to provide contrast between emulsions and silica components. TEM images in Figure 3 show that, upon increasing the reaction temperature, the emulsion droplet attached at one end of the rods shrank, as a result of the dissolution of water emulsions in pentanol due to increased solubility at elevated temperature.[14b] The temperature dependence of emulsion size was further confirmed by dynamic light scattering (DLS) analysis (Figure S7). DLS result shows that the size of emulsions containing all reagents except TEOS decreased with increasing temperature. Shrinkage of emulsion droplets causes a deviation from the center of the rod end and hence the formation of a curved segment. Formation of bent rods upon adding molecular sieves further confirms that the curved growth of silica rods is attributed to the shrinking of emulsion droplets (Figure S8). In contrast, during the synthesis of straight rods, the emulsion droplet maintains the same size and position throughout the synthesis.

Formation of BSRs can be induced by perturbing the pH of the reaction system also (Figure 4). After the growth of the first straight block, acetic acid (AcOH) was added into the system to lower the pH by neutralizing some of the NH_3. The perturbation

DOI: 10.1021/jacs.5b11546
J. Am. Chem. Soc. 2016, 138, 68−71

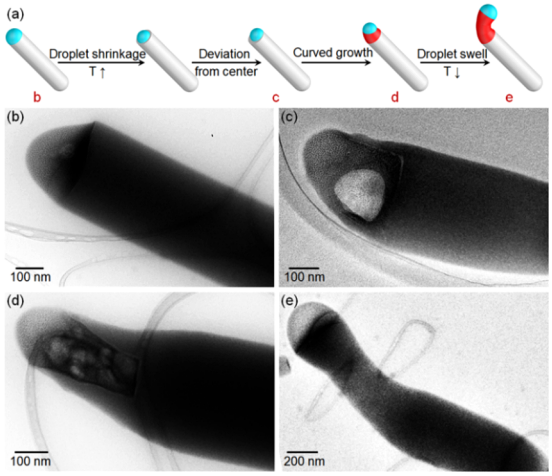

Figure 3. (a) Schematic illustration of the bending mechanism of BSRs based on the perturbation of emulsion droplet at elevated temperature. (b–e) TEM images of the rods at different growth stages with emulsion droplets attached at one end during the formation of BSRs: (b) rod grown at 25 °C for 2 h before temperature perturbation, (c,d) rod upon perturbation at 65 °C for (c) 1 min and (d) 5 min, and (e) rod in (d) that was further grown at 25 °C for 10 min.

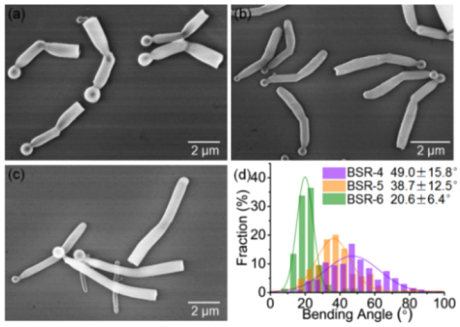

Figure 4. Representative SEM images of BSRs with different bending angles through pH modulation. Perturbation conditions were (a) pH 8.7 for 10 min for BSR-4, (b) pH 8.9 for 10 min for BSR-5, and (c) pH 9.3 for 20 min for BSR-6. Reaction conditions for growing two straight blocks of all the BSRs were pH 10.5 for 2 h before pH perturbation and pH 10.5 for 4 h after pH perturbation. (d) Bending angle distribution of BSR-4, BSR-5, and BSR-6 is obtained by counting 200 rods for each sample.

on pH induced curving of the rigid silica rods. We presume that this also arises from the shrinkage of emulsion droplets, which is confirmed by DLS measurement (Figure S9).[8a] The original reaction pH was restored for the further growth of the second straight block to produce BSRs by supplementing more NH_3 into the reaction system. The α value of the rods is strongly dependent on the strength of pH perturbation, that is, the amount of AcOH added into the reaction system. The larger the amount of AcOH added to induce perturbation (i.e., the lower the pH), the larger the α of the resulting BSRs. When 25 μL (0.44 mmol) of AcOH was added into ~7 mL of total solution with 0.48 mmol of NH_3 to perturb the reaction by reducing the pH from 10.5 to 8.7, ~92% of catalytic agent, NH_3, was neutralized. In this case, the resulting BSRs had an average $\alpha = 49.0 \pm 15.8°$ (Figure 4a,d). When the amount of AcOH was reduced to 20 μL (0.35 mmol) and the pH of the reaction system in the perturbation period of time was 8.9, the average α was reduced to $38.7 \pm 12.5°$ (Figure 4b,d). Further decreasing the amount (10 μL, 0.18 mmol) of added AcOH (i.e., a higher pH of 9.3) produced rods with an even smaller $\alpha = 20.6 \pm 6.4°$ (Figure 4c,d). However, when the pH of the reaction was below 8.6 upon the addition of excessive AcOH (27 μL, 0.48 mmol or more), most of the emulsion droplets were detached from the rods, leading to the termination of the growth of rods (Figure S10). The D of the second block was often slightly larger than that of the first block due to the addition of AcOH and NH_3 into the reaction system, which increased the emulsion droplet size (Figure 4a–c). When excess NH_3 was added for perturbation, the D of the second block increased dramatically (Figure S11). As temperature perturbation induced formation of BSRs, L of each arm of BSRs could be readily manipulated by controlling the incubation time during the growth of straight blocks. BSRs with variable $\alpha = 0–50°$ were generated through the pH-mediated strategy.

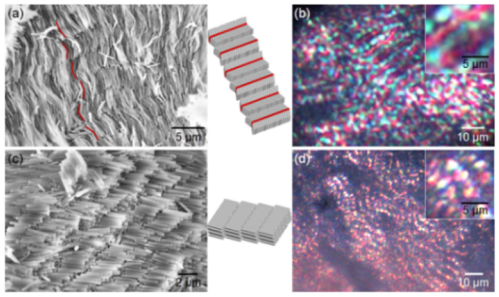

Figure 5. SEM and POM images of (a,b) BSRs (L_1 = 1500 nm, L_2 = 1500 nm, D = 200 nm, $\alpha = 35°$) and (c,d) straight rods (L = 2400 nm, D = 280 nm) after sedimentation. Insets: Enlarged POM images of assembled BSRs (b) and straight rods (d), respectively.

One of the most remarkable phenomena exhibited by colloidal suspensions of monodisperse rod-like particles is the spontaneous formation of smectic LCs.[11a] However, to our knowledge, the phase behavior of bent colloidal particles has not previously been explored theoretically or experimentally. We compared the LC phase behaviors of symmetrically bending BSRs and straight silica rods. A 30 vol% dispersion of BSRs or straight silica rods in dimethyl sulfoxide was sealed in glass capillary. The capillary was kept in a vertical position for 1 month to allow sedimentation. Compared with straight rods, it is striking that BSRs with $\alpha = 35°$ exhibit a typical synclinic tilted AF smectic bow phase (SmC_SP_A) in B2 phase after their sedimentation (Figure 5a,b). Figure 5a shows the representative scanning electron microscopy (SEM) image of the mesoscopic domains, where the BSRs closely align side-by-side, while the orientation direction (i.e., the polar direction) alternates from layer to layer, designated as AF structure. The tilting direction of the rod planes is uniform in most adjacent layers. As a result of the two different orientations of two segments of BSRs, the formation of SmC_SP_A phase is further confirmed by typical stripes with alternate colors running parallel to the layer planes in polarized optical microscopy (POM) images (Figures 5b and S12). The SmC_SP_A phase texture is in accordance with that of banana-shaped molecules[15] but has not previously been observed for colloidal particles. We presume that the SmC_SP_A phase can be explained by the macroscopic nonpolar property of the overall phase as well as the interlayer fluctuation of BSRs. In such a structure, driven by the excluded volume entropy, the BSRs are ordered in sterically compact packing arrangements on average, with the same bending directionality that restricts rotational freedom of rods.[17] Thus, there is an additional orientational order within each smectic layers. This gives rise to a spontaneous transverse polarization in the direction of the two-fold symmetry axis of the layer. The synclinic AF organization of

DOI: 10.1021/jacs.5b11546
J. Am. Chem. Soc. 2016, 138, 68–71

BSRs cancels the polarity between layers, thus leading to an energetically stable nonpolar overall structure. It also allows an easy out-of-plane interlayer fluctuation of the rods, stabilizing the structure in an entropic way. In contrast, SEM and POM images in Figure 5c,d reveal that straight rods with an aspect ratio of 8.5 form smectic C (SmC) phase after the slow sedimentation of rods (Figures 5d and S13). In the smectic phase, the rods order in periodic layers; on average, the long axes of the rods are tilted to the layer planes. This observation is in good agreement with previous report about the phase behavior of the silica rods with the aspect ratio of 8.[8b]

In summary, we developed a novel wet-chemical method to synthesize BSRs with well-controlled bending angle by introducing a temporary perturbation in temperature or pH during the growth of rods. To our knowledge, this is the first report of the synthesis of bending colloidal rods by using a wet-chemical method. It is remarkable that the BSRs behave like banana-shaped molecules to assemble into typical SmC_SP_A in B2 phase in the condensed phase, as a result of their specific bent shape. BSRs could serve as a new visual model for understanding the phase behavior of banana-shaped liquid crystals, and they may find applications in nonconventional photonic crystals or as templates for fabricating structural materials.[18]

■ ASSOCIATED CONTENT

Supporting Information

The Supporting Information is available free of charge on the ACS Publications website at DOI: 10.1021/jacs.5b11546.

Experiments and characterization; Figures S1−S13 (PDF)

■ AUTHOR INFORMATION

Corresponding Authors

*kliu@jlu.edu.cn

*znie@umd.edu

Notes

The authors declare no competing financial interest.

■ ACKNOWLEDGMENTS

Z.N. gratefully acknowledges financial support from the 3M Nontenured Faculty Award, grant R21DE024632A from National Institute for Dental & Craniofacial Research, and a startup fund from the University of Maryland. K.L. thanks National Natural Science Foundation of China (21474040, 21534004) and China's Thousand Talent Plan for financial support. Y.Y. acknowledges financial support from the International Postdoctoral Exchange Fellowship Program 2013 funded by the Office of China Postdoctoral Council (20130036), and China Postdoctoral Science Foundation (2013M540249, 2014-T70281). We also acknowledge support of the Maryland NanoCenter and its NispLab. The NispLab is supported in part by the NSF as a MRSEC Shared Experimental Facility.

■ REFERENCES

(1) (a) Vogel, N.; Retsch, M.; Fustin, C.-A.; del Campo, A.; Jonas, U. *Chem. Rev.* **2015**, *115*, 6265. (b) Manoharan, V. N. *Science* **2015**, *349*, 1253751.

(2) (a) Zhang, J.; Li, Y.; Zhang, X.; Yang, B. *Adv. Mater.* **2010**, *22*, 4249. (b) Li, F.; Josephson, D. P.; Stein, A. *Angew. Chem., Int. Ed.* **2011**, *50*, 360. (c) Wang, T.; LaMontagne, D.; Lynch, J.; Zhuang, J.; Cao, Y. C. *Chem. Soc. Rev.* **2013**, *42*, 2804. (d) Demirors, A. F.; Pillai, P. P.; Kowalczyk, B.; Grzybowski, B. A. *Nature* **2013**, *503*, 99. (e) de Nijs, B.; Dussi, S.; Smallenburg, F.; Meeldijk, J. D.; Groenendijk, D. J.; Filion, L.; Imhof, A.; van Blaaderen, A.; Dijkstra, M. *Nat. Mater.* **2015**, *14*, 56.

(3) (a) Galisteo-López, J. F.; Ibisate, M.; Sapienza, R.; Froufe-Pérez, L. S.; Blanco, Á.; López, C. *Adv. Mater.* **2011**, *23*, 30. (b) von Freymann, G.; Kitaev, V.; Lotsch, B. V.; Ozin, G. A. *Chem. Soc. Rev.* **2013**, *42*, 2528.

(4) Boncheva, M.; Whitesides, G. M. *MRS Bull.* **2005**, *30*, 736.

(5) (a) Park, S.; Lim, J.-H.; Chung, S.-W.; Mirkin, C. A. *Science* **2004**, *303*, 348. (b) Nie, Z.; Fava, D.; Kumacheva, E.; Zou, S.; Walker, G. C.; Rubinstein, M. *Nat. Mater.* **2007**, *6*, 609. (c) Mao, Z.; Xu, H.; Wang, D. *Adv. Funct. Mater.* **2010**, *20*, 1053. (d) Liu, K.; Nie, Z.; Zhao, N.; Li, W.; Rubinstein, M.; Kumacheva, E. *Science* **2010**, *329*, 197. (e) Chen, Q.; Whitmer, J. K.; Jiang, S.; Bae, S. C.; Luijten, E.; Granick, S. *Science* **2011**, *331*, 199. (f) Wang, Y.; Wang, Y.; Breed, D. R.; Manoharan, V. N.; Feng, L.; Hollingsworth, A. D.; Weck, M.; Pine, D. J. *Nature* **2012**, *491*, 51. (g) Li, Y.; Liu, Z.; Yu, G.; Jiang, W.; Mao, C. *J. Am. Chem. Soc.* **2015**, *137*, 4320.

(6) (a) Pusey, P. N.; van Megen, W. *Nature* **1986**, *320*, 340. (b) Anderson, V. J.; Lekkerkerker, H. N. W. *Nature* **2002**, *416*, 811. (c) Yethiraj, A. *Soft Matter* **2007**, *3*, 1099.

(7) (a) Glotzer, S. C.; Solomon, M. J. *Nat. Mater.* **2007**, *6*, 557. (b) Sacanna, S.; Pine, D. J.; Yi, G.-R. *Soft Matter* **2013**, *9*, 8096.

(8) (a) Kuijk, A.; van Blaaderen, A.; Imhof, A. *J. Am. Chem. Soc.* **2011**, *133*, 2346. (b) Kuijk, A.; Byelov, D. V.; Petukhov, A. V.; van Blaaderen, A.; Imhof, A. *Faraday Discuss.* **2012**, *159*, 181. (c) Lekkerkerker, H. N. W.; Vroege, G. J. *Philos. Trans. R. Soc., A* **2013**, *371*, 20120263. (d) Xu, T.; Davis, V. A. *Langmuir* **2014**, *30*, 4806. (e) Besseling, T. H.; Hermes, M.; Kuijk, A.; Nijs, B. d.; Deng, T. S.; Dijkstra, M.; Imhof, A.; van Blaaderen, A. *J. Phys.: Condens. Matter* **2015**, *27*, 194109. (f) He, J.; Yu, B.; Hourwitz, M. J.; Liu, Y.; Perez, M. T.; Yang, J.; Nie, Z. *Angew. Chem., Int. Ed.* **2012**, *51*, 3628. (g) Zhang, S.-Y.; Regulacio, M. D.; Han, M.-Y. *Chem. Soc. Rev.* **2014**, *43*, 2301.

(9) (a) Reddy, R. A.; Zhu, C.; Shao, R.; Korblova, E.; Gong, T.; Shen, Y.; Garcia, E.; Glaser, M. A.; Maclennan, J. E.; Walba, D. M.; Clark, N. A. *Science* **2011**, *332*, 72. (b) Cano, M.; Sánchez-Ferrer, A.; Serrano, J. L.; Gimeno, N.; Ros, M. B. *Angew. Chem., Int. Ed.* **2014**, *53*, 13449. (c) Kim, H.-J.; Jeong, Y.-H.; Lee, E.; Lee, M. *J. Am. Chem. Soc.* **2009**, *131*, 17371.

(10) (a) Ros, M. B.; Serrano, J. L.; de la Fuente, M. R.; Folcia, C. L. *J. Mater. Chem.* **2005**, *15*, 5093. (b) Reddy, R. A.; Tschierske, C. *J. Mater. Chem.* **2006**, *16*, 907. (c) Takezoe, H.; Takanishi, Y. *Jpn. J. Appl. Phys.* **2006**, *45*, 597. (d) Etxebarria, J.; Blanca Ros, M. *J. Mater. Chem.* **2008**, *18*, 2919.

(11) (a) Frenkel, D.; Lekkerkerker, H. N. W.; Stroobants, A. *Nature* **1988**, *332*, 822. (b) van der Kooij, F. M.; Kassapidou, K.; Lekkerkerker, H. N. W. *Nature* **2000**, *406*, 868. (c) Marechal, M.; Kortschot, R. J.; Demirörs, A. F.; Imhof, A.; Dijkstra, M. *Nano Lett.* **2010**, *10*, 1907.

(12) (a) Yu, N.; Genevet, P.; Kats, M. A.; Aieta, F.; Tetienne, J.-P.; Capasso, F.; Gaburro, Z. *Science* **2011**, *334*, 333. (b) Kauranen, M.; Zayats, A. V. *Nat. Photonics* **2012**, *6*, 737. (c) Ni, X.; Emani, N. K.; Kildishev, A. V.; Boltasseva, A.; Shalaev, V. M. *Science* **2012**, *335*, 427. (d) Kümmel, F.; ten Hagen, B.; Wittkowski, R.; Buttinoni, I.; Eichhorn, R.; Volpe, G.; Löwen, H.; Bechinger, C. *Phys. Rev. Lett.* **2013**, *110*, 198302. (e) Vercruysse, D.; Zheng, X.; Sonnefraud, Y.; Verellen, N.; Di Martino, G.; Lagae, L.; Vandenbosch, G. A. E.; Moshchalkov, V. V.; Maier, S. A.; Van Dorpe, P. *ACS Nano* **2014**, *8*, 8232. (f) ten Hagen, B.; Kümmel, F.; Wittkowski, R.; Takagi, D.; Löwen, H.; Bechinger, C. *Nat. Commun.* **2014**, *5*, 4829.

(13) Mirkovic, T.; Foo, M. L.; Arsenault, A. C.; Fournier-Bidoz, S.; Zacharia, N. S.; Ozin, G. A. *Nat. Nanotechnol.* **2007**, *2*, 565.

(14) (a) Zhang, J.; Liu, H.; Wang, Z.; Ming, N. *Chem. - Eur. J.* **2008**, *14*, 4374. (b) Datskos, P.; Sharma, J. *Angew. Chem., Int. Ed.* **2014**, *53*, 451.

(15) Link, D. R.; Natale, G.; Shao, R.; Maclennan, J. E.; Clark, N. A.; Körblova, E.; Walba, D. M. *Science* **1997**, *278*, 1924.

(16) Zhang, A.-Q.; Li, H.-J.; Qian, D.-J.; Chen, M. *Nanotechnology* **2014**, *25*, 135608.

(17) van Anders, G.; Klotsa, D.; Ahmed, N. K.; Engel, M.; Glotzer, S. C. *Proc. Natl. Acad. Sci. U. S. A.* **2014**, *111*, E4812.

(18) (a) Lu, Y.; Yin, Y.; Xia, Y. *Adv. Mater.* **2001**, *13*, 415. (b) Ding, T.; Song, K.; Clays, K.; Tung, C.-H. *Adv. Mater.* **2009**, *21*, 1936. (c) Shopsowitz, K. E.; Qi, H.; Hamad, W. Y.; MacLachlan, M. J. *Nature* **2010**, *468*, 422. (d) Wang, M.; He, L.; Xu, W.; Wang, X.; Yin, Y. *Angew. Chem., Int. Ed.* **2015**, *54*, 7077.

DOI: 10.1021/jacs.5b11546
J. Am. Chem. Soc. 2016, 138, 68−71